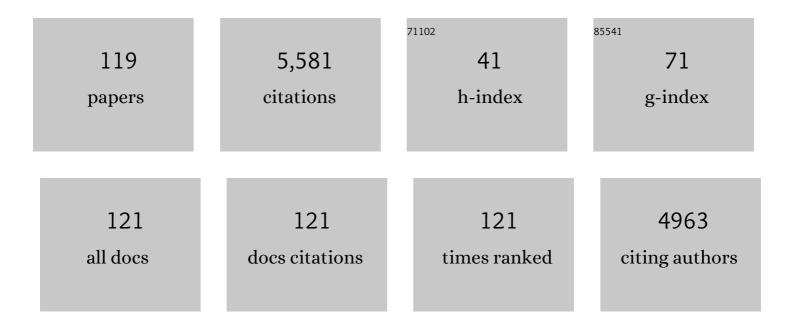
Vladimir V Galvita

List of Publications by Year in descending order

Source: https://exaly.com/author-pdf/2014961/publications.pdf Version: 2024-02-01



VIADIMIR V CALVITA

#	Article	IF	CITATIONS
1	Enhanced Carbon-Resistant Dry Reforming Fe-Ni Catalyst: RoleÂofÂFe. ACS Catalysis, 2015, 5, 3028-3039.	11.2	383
2	Super-dry reforming of methane intensifies CO ₂ utilization via Le Chatelier's principle. Science, 2016, 354, 449-452.	12.6	348
3	Ethane dehydrogenation on Pt/Mg(Al)O and PtSn/Mg(Al)O catalysts. Journal of Catalysis, 2010, 271, 209-219.	6.2	199
4	Catalyst performance of novel Pt/Mg(Ga)(Al)O catalysts for alkane dehydrogenation. Journal of Catalysis, 2010, 274, 200-206.	6.2	184
5	Carbon gasification from Fe–Ni catalysts after methane dry reforming. Applied Catalysis B: Environmental, 2016, 185, 42-55.	20.2	173
6	Production of hydrogen from dimethyl ether. Applied Catalysis A: General, 2001, 216, 85-90.	4.3	171
7	CeO ₂ -Modified Fe ₂ O ₃ for CO ₂ Utilization via Chemical Looping. Industrial & Engineering Chemistry Research, 2013, 52, 8416-8426.	3.7	149
8	Synthesis gas production by steam reforming of ethanol. Applied Catalysis A: General, 2001, 220, 123-127.	4.3	122
9	Catalyst-assisted chemical looping for CO2 conversion to CO. Applied Catalysis B: Environmental, 2015, 164, 184-191.	20.2	110
10	Steam reforming of glycerol: The experimental activity of La1â^'Ce NiO3 catalyst in comparison to the thermodynamic reaction equilibrium. Applied Catalysis B: Environmental, 2009, 90, 29-37.	20.2	104
11	Making chemicals with electricity. Science, 2019, 364, 734-735.	12.6	102
12	Delivering a Modifying Element to Metal Nanoparticles via Support: Pt–Ga Alloying during the Reduction of Pt/Mg(Al,Ga)O _{<i>x</i>} Catalysts and Its Effects on Propane Dehydrogenation. ACS Catalysis, 2014, 4, 1812-1824.	11.2	100
13	Solid electrolyte membrane reactors: Status and trends. Catalysis Today, 2005, 104, 185-199.	4.4	96
14	The Positive Role of Hydrogen on the Dehydrogenation of Propane on Pt(111). ACS Catalysis, 2017, 7, 7495-7508.	11.2	95
15	Bifunctional Ni-Ca based material for integrated CO2 capture and conversion via calcium-looping dry reforming. Applied Catalysis B: Environmental, 2021, 284, 119734.	20.2	91
16	Controlling the stability of a Fe–Ni reforming catalyst: Structural organization of the active components. Applied Catalysis B: Environmental, 2017, 209, 405-416.	20.2	89
17	Ethanol to higher hydrocarbons over Ni, Ga, Fe-modified ZSM-5: Effect of metal content. Applied Catalysis A: General, 2015, 492, 117-126.	4.3	88
18	Upgrading the value of anaerobic digestion <i>via</i> chemical production from grid injected biomethane. Energy and Environmental Science, 2018, 11, 1788-1802.	30.8	88

#	Article	IF	CITATIONS
19	Advanced Chemical Looping Materials for CO2 Utilization: A Review. Materials, 2018, 11, 1187.	2.9	85
20	Reaction network for the total oxidation of toluene over CuO–CeO2/Al2O3. Journal of Catalysis, 2011, 283, 1-9.	6.2	84
21	Nature of the active sites for the total oxidation of toluene by CuOCeO2/Al2O3. Journal of Catalysis, 2012, 295, 91-103.	6.2	78
22	The role of CO2 in the dehydrogenation of propane over WO –VO /SiO2. Journal of Catalysis, 2016, 335, 1-10.	6.2	77
23	Mg–Fe–Al–O for advanced CO ₂ to CO conversion: carbon monoxide yield vs. oxygen storage capacity. Journal of Materials Chemistry A, 2015, 3, 16251-16262.	10.3	70
24	Mechanism of CH4 Dry Reforming on Nanocrystalline Doped Ceria-Zirconia with Supported Pt, Ru, Ni, and Ni–Ru. Topics in Catalysis, 2013, 56, 958-968.	2.8	69
25	DFT-based microkinetic modeling of ethanol dehydration in H-ZSM-5. Journal of Catalysis, 2016, 339, 173-185.	6.2	69
26	Carbon capture and utilization in the steel industry: challenges and opportunities for chemical engineering. Current Opinion in Chemical Engineering, 2019, 26, 81-87.	7.8	67
27	Fe-Containing Magnesium Aluminate Support for Stability and Carbon Control during Methane Reforming. ACS Catalysis, 2018, 8, 5983-5995.	11.2	66
28	Deactivation of Modified Iron Oxide Materials in the Cyclic Water Gas Shift Process for CO-Free Hydrogen Production. Industrial & Engineering Chemistry Research, 2008, 47, 303-310.	3.7	65
29	Cyclic water gas shift reactor (CWGS) for carbon monoxide removal from hydrogen feed gas for PEM fuel cells. Chemical Engineering Journal, 2007, 134, 168-174.	12.7	63
30	Hydrogen production from methane by steam reforming in a periodically operated two-layer catalytic reactor. Applied Catalysis A: General, 2005, 289, 121-127.	4.3	61
31	CO2 conversion to CO by auto-thermal catalyst-assisted chemical looping. Journal of CO2 Utilization, 2016, 16, 8-16.	6.8	60
32	Hydrogen production by coal plasma gasification for fuel cell technology. International Journal of Hydrogen Energy, 2007, 32, 3899-3906.	7.1	58
33	Ultrafast and Stable CO ₂ Capture Using Alkali Metal Salt-Promoted MgO–CaCO ₃ Sorbents. ACS Applied Materials & Interfaces, 2018, 10, 20611-20620.	8.0	57
34	Deactivation Study of Fe ₂ O ₃ –CeO ₂ during Redox Cycles for CO Production from CO ₂ . Industrial & Engineering Chemistry Research, 2016, 55, 5911-5922.	3.7	56
35	CO production from CO 2 via reverse water–gas shift reaction performed in a chemical looping mode: Kinetics on modified iron oxide. Journal of CO2 Utilization, 2017, 17, 60-68.	6.8	56
36	Insights into the Reaction Mechanism of Ethanol Conversion into Hydrocarbons on Hâ€ZSMâ€5. Angewandte Chemie - International Edition, 2016, 55, 12817-12821.	13.8	52

#	Article	IF	CITATIONS
37	Catalyst-assisted chemical looping auto-thermal dry reforming: Spatial structuring effects on process efficiency. Applied Catalysis B: Environmental, 2018, 231, 123-136.	20.2	48
38	Redox behavior and reduction mechanism of Fe2O3–CeZrO2 as oxygen storage material. Journal of Materials Science, 2007, 42, 9300-9307.	3.7	46
39	Hydrogen and Carbon Monoxide Production by Chemical Looping over Ironâ€Aluminium Oxides. Energy Technology, 2016, 4, 304-313.	3.8	45
40	Atomic Layer Deposition Route To Tailor Nanoalloys of Noble and Non-noble Metals. ACS Nano, 2016, 10, 8770-8777.	14.6	44
41	Effect of Rh in Ni-based catalysts on sulfur impurities during methane reforming. Applied Catalysis B: Environmental, 2020, 267, 118691.	20.2	42
42	Combined chemical looping for energy storage and conversion. Journal of Power Sources, 2015, 286, 362-370.	7.8	41
43	A core-shell structured Fe 2 O 3 /ZrO 2 @ZrO 2 nanomaterial with enhanced redox activity and stability for CO 2 conversion. Journal of CO2 Utilization, 2017, 17, 20-31.	6.8	41
44	TAP study of toluene total oxidation over a Co ₃ O ₄ /La-CeO ₂ catalyst with an application as a washcoat of cordierite honeycomb monoliths. Physical Chemistry Chemical Physics, 2014, 16, 11447-11455.	2.8	40
45	Mechanism of carbon deposits removal from supported Ni catalysts. Applied Catalysis B: Environmental, 2018, 239, 502-512.	20.2	39
46	<i>110th Anniversary</i> : Carbon Dioxide and Chemical Looping: Current Research Trends. Industrial & Engineering Chemistry Research, 2019, 58, 16235-16257.	3.7	39
47	Effect of Boron Promotion on Coke Formation during Propane Dehydrogenation over Pt/γ-Al ₂ O ₃ Catalysts. ACS Catalysis, 2020, 10, 5208-5216.	11.2	39
48	Approaches for Selective Oxidation of Methane to Methanol. Catalysts, 2020, 10, 194.	3.5	38
49	Information-Driven Catalyst Design Based on High-Throughput Intrinsic Kinetics. Catalysts, 2015, 5, 1948-1968.	3.5	37
50	Study of butanol conversion to butenes over H-ZSM-5: Effect of chemical structure on activity, selectivity and reaction pathways. Applied Catalysis A: General, 2017, 539, 1-12.	4.3	37
51	Reciprocal relations between kinetic curves. Europhysics Letters, 2011, 93, 20004.	2.0	36
52	Bifunctional Co- and Ni- ferrites for catalyst-assisted chemical looping with alcohols. Applied Catalysis B: Environmental, 2018, 222, 59-72.	20.2	36
53	Fe-Based Nano-Materials in Catalysis. Materials, 2018, 11, 831.	2.9	36
54	Hydrogen Production from Methane and Carbon Dioxide by Catalyst-Assisted Chemical Looping. Topics in Catalysis, 2011, 54, 907-913.	2.8	34

#	Article	IF	CITATIONS
55	Production of hydrogen with low COx-content for PEM fuel cells by cyclic water gas shift reactor. International Journal of Hydrogen Energy, 2008, 33, 1354-1360.	7.1	33
56	Ethanol decomposition over Pd-based catalyst in the presence of steam. Reaction Kinetics and Catalysis Letters, 2002, 76, 343-351.	0.6	31
57	Formation and Functioning of Bimetallic Nanocatalysts: The Power of Xâ€ray Probes. Angewandte Chemie - International Edition, 2019, 58, 13220-13230.	13.8	31
58	The Role of Different Types of CuO in CuO–CeO2/Al2O3 for Total Oxidation. Catalysis Letters, 2014, 144, 32-43.	2.6	29
59	Unravelling the Formation of Pt–Ga Alloyed Nanoparticles on Calcined Ga-Modified Hydrotalcites by <i>in Situ</i> XAS. Chemistry of Materials, 2014, 26, 5936-5949.	6.7	28
60	Advanced Elemental Characterization during Pt–In Catalyst Formation by Wavelet Transformed X-ray Absorption Spectroscopy. Analytical Chemistry, 2015, 87, 3520-3526.	6.5	28
61	3D-printing of metallic honeycomb monoliths as a doorway to a new generation of catalytic devices: the Ni-based catalysts in methane dry reforming showcase. Catalysis Communications, 2021, 148, 106181.	3.3	28
62	Kinetics of chemical processes: From molecular to industrial scale. Journal of Catalysis, 2021, 404, 745-759.	6.2	28
63	Early stages in the formation and burning of graphene on a Pt/Mg(Al)O dehydrogenation catalyst: A temperature- and time-resolved study. Journal of Catalysis, 2016, 344, 482-495.	6.2	27
64	The role of hydrogen during Pt–Ga nanocatalyst formation. Physical Chemistry Chemical Physics, 2016, 18, 3234-3243.	2.8	27
65	Local environment of Fe dopants in nanoscale Fe : CeO _{2â^'x} oxygen storage material. Nanoscale, 2015, 7, 3196-3204.	5.6	26
66	FeO controls the sintering of iron-based oxygen carriers in chemical looping CO2 conversion. Journal of CO2 Utilization, 2020, 40, 101216.	6.8	26
67	Exploring the stability of Fe2O3-MgAl2O4 oxygen storage materials for CO production from CO2. Journal of CO2 Utilization, 2019, 29, 36-45.	6.8	25
68	Looking inside a Ni-Fe/MgAl2O4 catalyst for methane dry reforming via Mössbauer spectroscopy and in situ QXAS. Applied Catalysis B: Environmental, 2022, 300, 120720.	20.2	25
69	Role of intermediates in reaction pathways from ethene to hydrocarbons over H-ZSM-5. Applied Catalysis A: General, 2017, 538, 207-220.	4.3	24
70	Ethanol dehydrogenation over Cu catalysts promoted with Ni: Stability control. Applied Catalysis A: General, 2020, 591, 117401.	4.3	24
71	An alternative method for parameter identification from temperature programmed reduction (TPR) data. Chemical Engineering Science, 2008, 63, 4776-4788.	3.8	22
72	Hierarchical Fe-modified MgAl ₂ O ₄ as a Ni-catalyst support for methane dry reforming. Catalysis Science and Technology, 2020, 10, 6987-7001.	4.1	22

#	Article	IF	CITATIONS
73	Ni nanoparticles and the Kirkendall effect in dry reforming of methane. Applied Surface Science, 2018, 452, 239-247.	6.1	21
74	Pressure-induced deactivation of core-shell nanomaterials for catalyst-assisted chemical looping. Applied Catalysis B: Environmental, 2019, 247, 86-99.	20.2	21
75	What Makes Fe-Modified MgAl ₂ O ₄ an Active Catalyst Support? Insight from X-ray Raman Scattering. ACS Catalysis, 2020, 10, 6613-6622.	11.2	21
76	Thermodynamic time-invariances: Theory of TAP pulse-response experiments. Chemical Engineering Science, 2011, 66, 4683-4689.	3.8	20
77	Ethanol dehydration pathways in H-ZSM-5: Insights from temporal analysis of products. Catalysis Today, 2020, 355, 822-831.	4.4	20
78	One-pot synthesis of Pt catalysts based on layered double hydroxides: an application in propane dehydrogenation. Catalysis Science and Technology, 2016, 6, 1863-1869.	4.1	19
79	Reprint of "Ethanol to higher hydrocarbons over Ni, Ga, Fe-modified ZSM-5: Effect of metal content― Applied Catalysis A: General, 2015, 504, 621-630.	4.3	17
80	Fe ₂ O ₃ –MgAl ₂ O ₄ for CO Production from CO ₂ : MA¶ssbauer Spectroscopy and in Situ X-ray Diffraction. ACS Sustainable Chemistry and Engineering, 2019, 7, 9553-9565.	6.7	17
81	Microstructured ZrO2 coating of iron oxide for enhanced CO2 conversion. Applied Catalysis B: Environmental, 2021, 292, 120194.	20.2	17
82	Momentary Equilibrium in Transient Kinetics and Its Application for Estimating the Concentration of Catalytic Sites. Industrial & Engineering Chemistry Research, 2013, 52, 15417-15427.	3.7	16
83	PdZn nanoparticle catalyst formation for ethanol dehydrogenation: Active metal impregnation vs incorporation. Applied Catalysis A: General, 2018, 555, 12-19.	4.3	16
84	CO2 sorption properties of Li4SiO4 with a Li2ZrO3 coating. Journal of CO2 Utilization, 2019, 34, 688-699.	6.8	16
85	Microkinetics for toluene total oxidation over CuO–CeO2/Al2O3. Catalysis Today, 2015, 258, 214-224.	4.4	15
86	Kinetics of Lifetime Changes in Bimetallic Nanocatalysts Revealed by Quick Xâ€ray Absorption Spectroscopy. Angewandte Chemie - International Edition, 2018, 57, 12430-12434.	13.8	15
87	In Situ XAS/SAXS Study of Al ₂ O ₃ -Coated PtGa Catalysts for Propane Dehydrogenation. ACS Catalysis, 2021, 11, 11320-11335.	11.2	15
88	Coupling CO2 utilization and NO reduction in chemical looping manner by surface carbon. Applied Catalysis B: Environmental, 2021, 297, 120472.	20.2	14
89	Insight in kinetics from preâ€edge features using time resolved <i>in situ</i> XAS. AICHE Journal, 2018, 64, 1339-1349.	3.6	13
90	Exceeding Equilibrium CO ₂ Conversion by Plasma-Assisted Chemical Looping. ACS Energy Letters, 2022, 7, 1896-1902.	17.4	13

#	Article	IF	CITATIONS
91	The CO adsorption on a Fe2O3–Ce0.5Zr0.5O2 catalyst studied by TPD, isotope exchange and FTIR spectroscopy. Journal of Molecular Catalysis A, 2008, 283, 43-51.	4.8	12
92	Structural and Kinetic Study of the Reduction of CuO–CeO2/Al2O3 by Time-Resolved X-ray Diffraction. Catalysis Letters, 2012, 142, 959-968.	2.6	12
93	Size- and composition-controlled Pt–Sn bimetallic nanoparticles prepared by atomic layer deposition. RSC Advances, 2017, 7, 20201-20205.	3.6	12
94	Formation and stability of an active PdZn nanoparticle catalyst on a hydrotalcite-based support for ethanol dehydrogenation. Catalysis Science and Technology, 2017, 7, 3715-3727.	4.1	12
95	Precise non-steady-state characterization of solid active materials with no preliminary mechanistic assumptions. Catalysis Today, 2017, 298, 203-208.	4.4	11
96	Carbon monoxide production using a steel mill gas in a combined chemical looping process. Journal of Energy Chemistry, 2022, 68, 811-825.	12.9	11
97	Insights into the Reaction Mechanism of Ethanol Conversion into Hydrocarbons on Hâ€ZSMâ€5. Angewandte Chemie, 2016, 128, 13009-13013.	2.0	10
98	Combined Chemical Looping: New Possibilities for Energy Storage and Conversion. Energy & Fuels, 2017, 31, 11509-11514.	5.1	10
99	Designing Nanoparticles and Nanoalloys for Gas-Phase Catalysis with Controlled Surface Reactivity Using Colloidal Synthesis and Atomic Layer Deposition. Molecules, 2020, 25, 3735.	3.8	10
100	Intensifying blue hydrogen production by in situ CO2 utilisation. Journal of CO2 Utilization, 2022, 61, 102014.	6.8	9
101	Performance of a SOFC fed by ethanol reforming products. Solid State Ionics, 2002, 152-153, 551-554.	2.7	8
102	Kinetics of Multi‣tep Redox Processes by Timeâ€Resolved In Situ Xâ€ray Diffraction. Chemie-Ingenieur-Technik, 2016, 88, 1684-1692.	0.8	8
103	Behaviour of Platinum-Tin during CO2-assisted propane dehydrogenation: Insights from quick X-ray absorption spectroscopy. Journal of Catalysis, 2022, 408, 356-371.	6.2	8
104	Intensification of Chemical Looping Processes by Catalyst Assistance and Combination. Catalysts, 2021, 11, 266.	3.5	7
105	Formation and Functioning of Bimetallic Nanocatalysts: The Power of Xâ€ray Probes. Angewandte Chemie, 2019, 131, 13354-13364.	2.0	6
106	First-Principles-Based Simulation of an Industrial Ethanol Dehydration Reactor. Catalysts, 2019, 9, 921.	3.5	6
107	Impact of the Spatial Distribution of Active Material on Bifunctional Hydrocracking. Industrial & Engineering Chemistry Research, 2021, 60, 6357-6378.	3.7	6
108	Decarbonisation of steel mill gases in an energy-neutral chemical looping process. Energy Conversion and Management, 2022, 254, 115248.	9.2	6

#	Article	IF	CITATIONS
109	How Does the Surface Structure of Ni-Fe Nanoalloys Control Carbon Formation During Methane Steam/Dry Reforming?. , 2019, , 177-225.		5
110	Spherical core–shell alumina support particles for model platinum catalysts. Nanoscale, 2021, 13, 4221-4232.	5.6	5
111	Separate H ₂ and CO production from CH ₄ O ₂ cycling of Feâ€Ni. AICHE Journal, 0, , .	3.6	3
112	Preferential Oxidation of H ₂ in CO-Rich Streams over a Ni/γ-Al ₂ O ₃ Catalyst: An Experimental and First-Principles Microkinetic Study. ACS Catalysis, 0, , 9011-9022.	11.2	3
113	Kinetics of Lifetime Changes in Bimetallic Nanocatalysts Revealed by Quick Xâ€ray Absorption Spectroscopy. Angewandte Chemie, 2018, 130, 12610-12614.	2.0	2
114	Upcycling the carbon emissions from the steel industry into chemicals using three metal oxide loops. Energy Advances, 2022, 1, 367-384.	3.3	2
115	(Invited) Atomic Layer Deposition of Nanoalloys of Noble and Non-Noble Metals. ECS Transactions, 2017, 80, 97-106.	0.5	1
116	Trimetallic Catalyst Configuration for Syngas Production. ChemCatChem, 0, , .	3.7	1
117	Shadowing Effect in Catalyst Activity: Experimental Observation. ACS Catalysis, 2022, 12, 5455-5463.	11.2	1
118	Aligning time-resolved kinetics (TAP) and surface spectroscopy (AP-XPS) for a more comprehensive understanding of ALD-derived 2D and 3D model catalysts Faraday Discussions, 2022, , .	3.2	0
119	TAP analysis of single and double peak responses during CO oxidation over Pt. Catalysis Today, 2022, , .	4.4	Ο